Theoretical study of cation–π interaction in graphene fragments

Jorge A. Carrazana-García[1]*, Enrique M. Cabaleiro-Lago[1] and Jesús Rodríguez-Otero[2]

[1] Departamento de Química Física, Facultade de Ciencias, Universidade de Santiago de Compostela. Campus de Lugo. Avenida Alfonso X El Sabio s/n, Lugo 27002, Spain.

[2] Departamento de Química Física, Facultade de Química, Universidade de Santiago de Compostela, Santiago de Compostela 15782, Spain.

* *Correspondence*: jorge.carrazana@usc.com

Abstract:

The interaction between cations and delocalized electronic clouds (the cation-π interaction) occupies a very important place within non-binding interactions. Its presence has long been recognized as fundamental for both, the structure and function, of proteins and other important biological molecules. Rechargeable batteries and fuel cells industries are also interested in cation-π interaction and the use of graphene and similar carbon allotropes are investigated as promising alternatives in their technological applications. Reliable and practically applicable theoretical models of cation-π interaction are needed for guiding these researches. In this work, the interaction of cations (Li^+, Na^+, K^+, ammonium and guanidinium) with graphene fragments (from benzene to circumcoronene) is modeled using DFT level of theory. Linear scans (TPSS+D3/Def2TZVPP) that follow trajectories perpendicular to the central ring of the graphene fragments allow the location of the distance at which the strongest interaction takes place. Using the geometry of the minima, the interaction energy is decomposed in physically meaningful contributions using a SAPT(DFT) method. It is observed that benzene complexes systematically deviate from the trend followed by complexes with larger fragments, so this system does not constitute a good model for the study of cation-π interaction in graphenes or other large conjugated molecules. While induction is the main contribution in complexes with Li^+ and Na^+, the stability of most of the complexes investigated depends on a balanced combination of the three contributions: electrostatic, induction and dispersion. Following the tendencies observed with organic fragments with an increasing number of conjugated rings, the results can be extrapolated to extended π-systems as graphene.

1. Introduction

The cation-π interaction is a very important non-covalent interaction because of its presence in several fields of chemistry, biology and industry. Many inclusion complexes and other supramolecular structures are formed via cation-π contacts.[1,2] The participation of cation-π interactions in catalysis includes the stabilization of reactive intermediates and transition states.[3,4] This interaction plays a central role both in the function and in the structure[5,6] of proteins and other macromolecules[7,8] and determines the action of enzymes,[9] biological receptors[10] and ionic channels.[11] The understanding that adhesion of mussel proteins to underwater surfaces occurs via cation–π interactions in aqueous media[12] provided new insights for the development of biomimetic underwater adhesives. Recently it has been reported that the presence of alkali metal cations in carbonaceous adsorbents intensifies the adsorption of hydrogen.[13] As well, the replacement of metal electrodes by lithium inserted in carbon-based anodes allowed the production of safer Li-metal ion rechargeable batteries.[14] These findings stimulate the interest of the rechargeable batteries and fuel cells industries in cation-π interaction.

From the theoretical point of view, understanding the nature of a cation-π interaction is essential for its introduction into reliable and accurate classical force fields used in a wide sort of areas ranging from biomolecule simulations[15] and drug design investigations[16] to the modeling of metallic-doped carbon cathodes[17] and graphene-based membranes.[18] Since the discovering of this interaction many theoretical approaches explaining its physical origin have been devised.[19] The interaction of the cation with the large, permanent quadrupole moment of aromatic rings was initially established as the driving force of the cation-π interaction.[20,21,22] Other investigations revealed that repulsion and induction contributions are important too.[23,24] Finally, the recognition that also dispersion plays a very important role in the stability of cation-π complexes of practical interest[25] serves as a guide for their study, indicating that a proper description of dispersive effects is required in their theoretical investigation.

In this study, the interaction of some metallic and organic cations with planar conjugated molecules that model graphene fragments of increasing size is theoretically investigated using DFT level of theory with an empirical description of dispersion. For gaining understanding in the nature of the cation-π interaction a rigorous method of energy analysis is also applied, separating the interaction energy in physically meaningful contributions. The results obtained with organic fragments with an increasing number of conjugated rings can be extrapolated to extended π-systems as graphene.

2. Methods

The structure of the polyatomic cations (Fig.1) and the graphene fragments (Fig. 2) were optimized at the TPSS+D3/Def2TZVPP level of theory using the Gaussian 09 suite of programs,[26] confirming that the stationary points found in the potential energy surface correspond to minima (frequency calculations were avoided in the case of B19 = circumcoronene due to resource limitations). The same level of calculation and program were used in the computation of the Molecular Electrostatic Potential (Figs. 2 and 3). The cation-π interaction was first studied by rigid scans performed by moving the cation along a path that passes through the molecular center and that it is perpendicular to the plane of the graphene fragment. The orientations of the polyatomic cations during these scans are shown in Fig. 1. BSSE-free interaction energies were computed with the ORCA (ver 3.0.3) electronic structure package[27] using the supermolecule approach also at the

TPSS+D3/Def2TZVPP level of calculation. Once the potential curves for the dimers are available, the positions of the minima are obtained by interpolation. Using the cation – graphene fragment separation corresponding to the minima found in the scans, physically significant contributions to the interaction energy were obtained using the symmetry-adapted perturbation theory with intramonomer correlation effects described at the DFT level SAPT(DFT)[28,29,30,31] implemented in MOLPRO (ver. 2015.1). [32] This energy analysis was performed at the PBE0/cc-pVDZ and PBE0/cc-pVTZ levels of calculation. The contributions obtained from SAPT are grouped into four terms, corresponding to repulsion, electrostatic, induction, and dispersion contributions. It is considered that $Rep = E^1_{exch}$; $Elec = E^1_{pol}$; $Ind = E^2_{ind} + E^2_{exch-ind} + \delta_{HF}$; $Disp = E^2_{disp} + E^2_{exch-disp}$. δ_{HF} is a term representing contributions higher than second order and it is obtained from a SAPT calculation employing Hartree–Fock wavefunctions: $\delta_{HF} = \Delta E_{HF} - (E^1_{exch} + E^1_{pol} + E^2_{ind} + E^2_{exch-ind})$, with ΔE_{HF} being the counterpoise- corrected interaction energy at the HF level. While most contributions to the interaction energy already reach values close to the basis set limit with a basis set of triple-zeta quality, dispersion contribution converges very slowly with the basis set size. Therefore, dispersion values are extrapolated to the basis set limit assuming a cubic dependence as suggested by Helgaker employing cc-pVDZ and cc-pVTZ basis sets.[33,34] Thus, the final SAPT(DFT) values are a combination of the cc-pVTZ electrostatic, repulsion, and induction contributions, plus the dispersion contribution extrapolated to basis limit.[35,36,37]
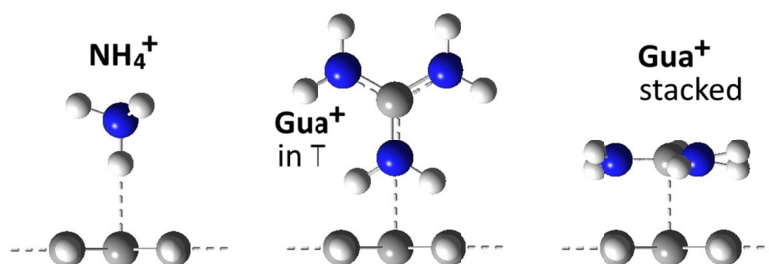
Figure 1. Organic cations: NH_4^+ = ammonium and Gua^+ = guanidinium, showing their orientations respect to the graphene fragments studied.

3. Results and Discussion

The structures of the conjugated molecules employed in this study for representing graphene fragments of increasing size are presented in Fig. 2 along with the Molecular Electrostatic Potential (MEP) distribution around each molecule. Cations are electrostatically attracted by the π-cloud and this interaction is the primary cause for de formation of cation-π complexes. The (negative) value of the electrostatic potential of the π-cloud is influenced by the size of the molecule that in this family can be quantified by the number of benzene rings in each molecule.

MEP values calculated following the line normal to the central ring of the molecules of Fig. 2 are represented in Fig. 3 as a function of the distance to the plane of the molecule. In each trajectory the coordinates of the minimum are determined by interpolation. As it can be observed in the inset of Fig. 3, there is an important influence of the size of the π-systems on the position and on the depth of the MEP profiles, indicating that small molecules (anthracene and, mainly, benzene) are not good models for extended graphene fragments. For molecules with four or more benzene rings the minimum MEP value in the trajectory studied approaches slowly to around -8 … -9 kcal/mol.
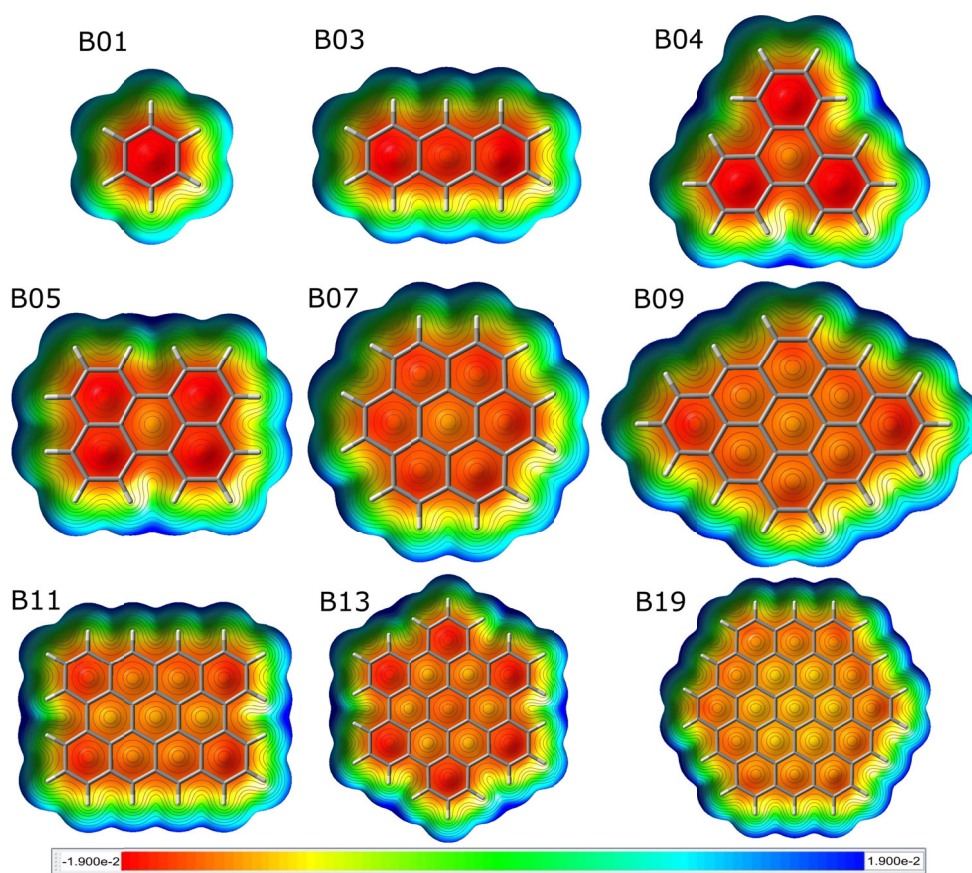
Figure 2. Structure of the molecules used in this study as models of graphene fragments. The acronym used to identify the molecule reflects the number of benzene rings in its structure. For each molecule the distribution of the Molecular Electrostatic Potential (MEP) mapped on the electronic density isosurface of 0.0004 a.u. is also shown.
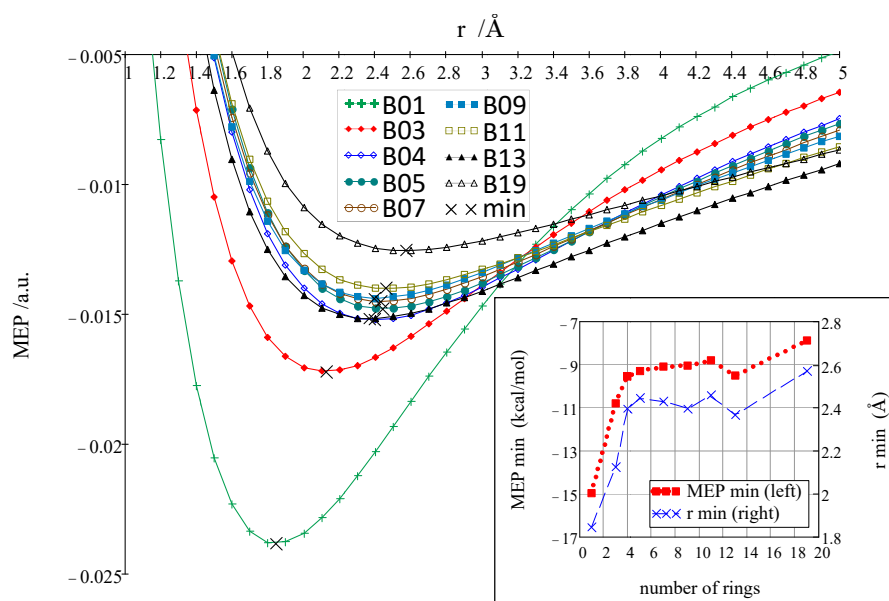
Figure 3. Molecular electrostatic potential (MEP) along the line normal to the central ring of graphene fragments as a function of r, the distance to the plane of the molecule. This line is also the trajectory followed by the cations in the scans shown in Fig. 4. The position and the energy of the MEP minima ordered by the number of benzene rings in the graphene fragments are presented in the inset.

The energy of the interaction between the molecules of Fig. 2 and the cations studied are shown in the left-side plots of both columns of Fig. 4. The interaction energy and the separation between the cation and the π-system corresponding to the minima of these representations are listed in Table I and represented in the right-side plots of both columns of Fig. 4. In all the cases very stable cation-π complexes are formed and, for a particular cation, the stability of the complex increases with the size of the conjugate molecule. The separation between the cation and the conjugated molecule in the minima of the scans decreases slightly with the extent of the π-system, corresponding to the formation of increasingly stable complexes as the graphene fragment grows. As expected from the MEP study, complexes with benzene are clearly apart from the complexes formed by the bigger conjugated molecules. For graphene fragments with four or more benzene rings the interaction energies of the complexes are grouped within a window of 3 to 5 kcal/mol, and for B13 and B19 the E_{int} value can be considered stabilized. The same is observed in the cation – π-system separation in the minima of E_{int}.

Thanks to its strong polarizing power, the more stable complexes are formed by Li$^+$. As the cation size increases the contribution of induction is lower and for bigger cations E_{int} is progressively less negative. This tendency is kept in the complexes with organic cations but when comparing the same cation, guanidinium, in two different orientations it is observed that the complexes in the stacked configuration are more stable than the corresponding complexes with the configuration "in T". This reveals the importance of another contribution which plays a minor role in the cases previously analyzed: dispersion.

Table I. Coordinates of the minima found in the TPSS-D3/Def2TZVPP scans. These values are represented in the right-side plots of both columns in Fig. 4 as function of the size of the π-system.

E_{int} / kcal·mol^{-1} r (cat⋯π) / Å	B01	B03	B04	B05	B07	B09	B11	B13	B19
Li$^+$	-38.98	-43.57	-43.92	-44.01	-45.41	-47.70	-48.91	-51.20	-50.55
	1.84	1.80	1.80	1.80	1.80	1.79	1.78	1.77	1.77
Na$^+$	-24.81	-29.02	-30.54	-30.96	-31.53	-33.02	-34.18	-35.68	-35.44
	2.45	2.37	2.34	2.33	2.33	2.32	2.31	2.31	2.31
K$^+$	-16.94	-21.15	-22.88	-23.22	-23.81	-25.08	-26.02	-27.33	-27.14
	2.89	2.79	2.76	2.76	2.77	2.75	2.74	2.74	2.74
NH$_4$$^+$	-18.92	-23.14	-24.66	-24.97	-25.76	-27.22	-28.23	-29.80	-29.50
	2.98	2.91	2.89	2.89	2.89	2.88	2.87	2.86	2.87
Gua$^+$ in T	-10.74	-14.07	-15.86	-16.46	-16.75	-17.71	-18.57	-19.64	-19.64
	4.37	4.27	4.23	4.22	4.23	4.22	4.21	4.20	4.20
Gua$^+$ stacked	-7.47	-13.61	-16.95	-17.74	-19.21	-20.37	-21.41	-22.54	22.90
	3.57	3.29	3.23	3.20	3.19	3.18	3.18	3.18	3.17

To quantify more precisely the importance of the different contributions to E_{int} and gaining understanding about the nature of the cation-π in these complexes, the SAPT(DFT) energy analysis procedure is applied. With this method and using the cation – π-system separation corresponding to the minima found in the scans of Fig. 4, the interaction energy is separated in its repulsion, electrostatic, induction and dispersion contributions. The results of the energy analysis are presented in Table II and in Fig. 5.

Figure 4. For both columns: *Left* = interaction energy as function of the distance between the cations and the π-system. Only the points around the minimum of each dependency are shown. In all the cases the trajectory explored is perpendicular to the center of the graphene fragment. *Right* = position and interaction energy corresponding to the minima found in the scans, ordered by the number of benzene rings in the graphene fragment.

The only destabilizing contribution in all of these cases is repulsion, which values (not considering the complexes with benzene) are grouped in the 8 to 14 kcal/mol range. The trends observed by E_{int} are determined mainly by the balance between the stabilizing contributions. As in most of cation-π complexes, the electrostatic contribution is important in all of these systems, but induction is the leading contribution to the stability in the complexes formed by Li^+, Na^+, K^+ and NH_4^+. Complexes formed by the guanidinium cation perpendicular to the conjugated molecule (configuration "in T") owe their stability to a combination of electrostatic, induction and dispersion that contribute in almost the same proportion. Dispersion, that has a minor effect in the complexes formed by Li^+ and Na^+, is an important contribution in the complexes with K^+ and bigger cations, especially in the complexes formed by the guanidinium cation in the stacked configuration.

The influence of the π-system size is observed mostly in induction: as the conjugated molecule grows, its polarizability increases and the value of the induction contribution becomes more negative. This is reflected in the interaction energy values but when the conjugated molecule has 13 – 19 benzene rings the values of E_{int} and its contributions can be considered essentially stabilized.

Table II. Interaction energy analysis performed with the SAPT(DFT) method using the geometries of the minima found in the scans presented in Fig. 4.

	B01	B03	B04	B05	B07	B09	B11	B13	B19
					Li^+				
r	1.84	1.82	1.82	1.82	1.82	1.81	1.78	1.79	1.77
Eint	-38.35	-42.38	-42.11	-42.11	-43.04	-45.80	-46.62	-49.15	-47.70
Rep	12.74	12.57	11.79	11.99	12.35	12.83	13.95	13.64	14.37
Elec	-17.83	-13.34	-10.62	-10.28	-10.21	-10.49	-9.59	-10.78	-7.67
Ind	-32.17	-40.46	-42.16	-42.69	-43.99	-46.90	-49.67	-50.71	-53.04
Disp	-1.10	-1.16	-1.13	-1.13	-1.19	-1.24	-1.31	-1.30	-1.36
					Na^+				
r	2.42	2.38	2.36	2.36	2.37	2.36	2.36	2.35	2.31
Eint	-23.13	-27.08	-28.32	-28.78	-28.92	-30.49	-31.73	-32.68	-32.17
Rep	7.90	8.14	7.97	8.00	8.02	8.41	8.36	8.78	9.81
Elec	-15.30	-13.83	-12.86	-12.71	-12.41	-12.58	-12.31	-12.66	-11.00
Ind	-14.85	-20.38	-22.38	-23.00	-23.44	-25.19	-26.65	-27.63	-29.72
Disp	-0.89	-1.02	-1.06	-1.07	-1.09	-1.13	-1.13	-1.17	-1.27
					K^+				
r	2.84	2.77	2.74	2.74	2.75	2.74	2.73	2.72	2.74
Eint	-17.60	-21.79	-23.34	-23.70	-23.97	-25.49	-26.55	-27.55	-27.14
Rep	9.16	10.27	10.43	10.45	10.39	10.88	11.16	11.71	10.86
Elec	-13.34	-13.22	-13.08	-13.03	-12.71	-12.88	-12.86	-13.20	-11.37
Ind	-10.10	-14.77	-16.37	-16.75	-17.20	-18.88	-20.15	-21.22	-21.89
Disp	-3.31	-4.07	-4.33	-4.37	-4.45	-4.61	-4.71	-4.85	-4.74
					NH_4^+				
r	2.97	2.91	2.90	2.90	2.90	2.88	2.88	2.87	2.87
Eint	-17.89	-21.62	-22.74	-22.97	-23.62	-25.29	-26.21	-27.42	-27.37
Rep	11.42	12.61	12.25	12.31	12.60	13.47	13.43	13.95	13.85
Elec	-12.20	-12.00	-11.70	-11.58	-11.63	-11.95	-11.86	-12.24	-11.12
Ind	-11.52	-15.63	-16.54	-16.91	-17.57	-19.45	-20.39	-21.54	-22.46
Disp	-5.58	-6.60	-6.75	-6.80	-7.02	-7.36	-7.39	-7.59	-7.64
					Gua^+ in T				
r	4.37	4.29	4.25	4.24	4.26	4.24	4.23	4.24	4.20
Eint	-10.22	-13.3	-14.92	-15.5	-15.69	-16.76	-17.4	-18.52	-18.52
Rep	8.09	9.47	9.98	10.23	9.81	10.57	10.85	10.70	11.94
Elec	-8.09	-8.80	-9.49	-9.81	-9.49	-9.91	-9.92	-10.51	-10.12
Ind	-5.01	-7.27	-8.03	-8.32	-8.37	-9.38	-10.09	-10.47	-11.49
Disp	-5.21	-6.71	-7.38	-7.60	-7.63	-8.05	-8.25	-8.25	-8.86
					Gua^+ stacked				
r	3.49	3.27	3.21	3.19	3.16	3.16	3.16	3.15	3.17
Eint	-6.99	-13.22	-16.35	-17.17	-18.60	-19.82	-20.69	-21.73	-20.95
Rep	5.15	9.96	12.03	12.57	13.48	13.58	13.65	14.20	13.22
Elec	-4.96	-9.60	-11.97	-12.52	-13.24	-13.34	-13.46	-14.07	-13.01
Ind	-1.93	-4.27	-5.34	-5.67	-6.25	-7.22	-7.87	-8.55	-9.20
Disp	-5.25	-9.31	-11.08	-11.55	-12.59	-12.85	-13.01	-13.31	-11.95

Figure 5. Analysis of the interaction energy of the complexes formed between the graphene fragments and the cations studied. The interaction energy and its repulsion, electrostatic, induction and dispersion contributions are plotted in function of the number of benzene rings in the graphene fragments.

The relative importance of induction, electrostatic and dispersion to the stability of the complexes studied is emphasized in the triangular plot of Fig. 6. For each system, the electrostatic contribution is transformed in the %Elec coordinate calculated as follow:

$$\%\text{Elec} = \frac{\text{Elec} \cdot 100\%}{\text{Elec} + \text{Ind} + \text{Disp}}$$
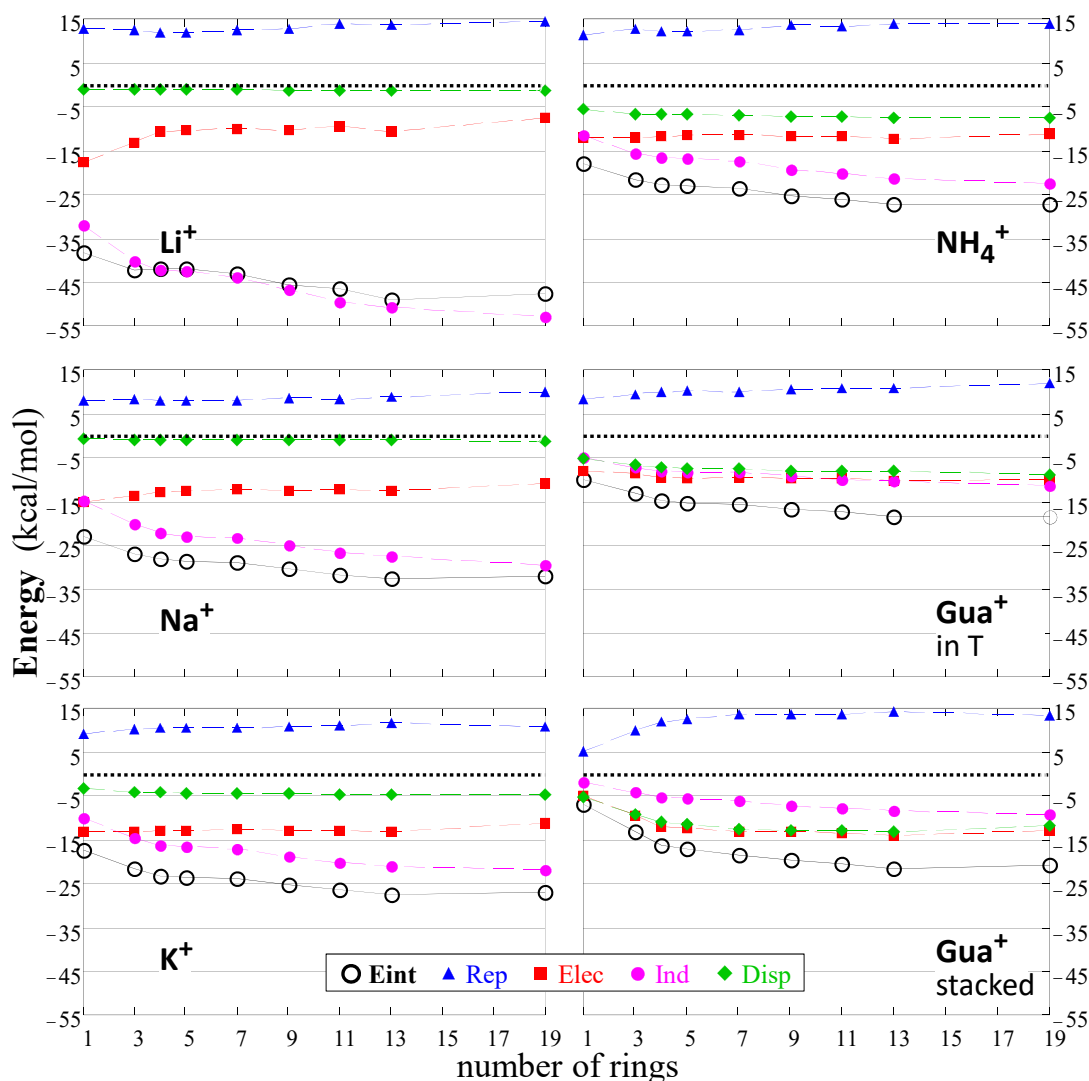
This coordinate transformation is applied similarly to induction and dispersion and the points are represented in the triangular plot. In Fig. 6 it can be observed that the complexes of the different cations are clearly grouped in clusters. Dispersion has a minor effect in the stability of Li^+ and Na^+ complexes, but confers more than 10% of the stability to the K^+ complexes, about the 20% to the NH_4^+ complexes and 30% to the guanidinium complexes with the configuration "in T". The clusters of points corresponding to all of these cations are located almost parallel to the Ind – Elec side of the plot, indicating that the proportional effect of dispersion in the stability is essentially the same in the complexes of Li^+, Na^+, K^+ and NH_4^+ cations with conjugated molecules of different number of

benzene rings. The effect of the size of the π-system in the stability of these complexes consists in the progressive interchange between the role of electrostatic (more important in the smaller π-systems) and induction (more important in the extended π-systems). For the complexes with guanidinium in the stacked configuration the dispersion contribution is even more important than for the complexes analyzed previously and the effect of the size of the π-system is also more complicated but systematic.

Among the 54 complexes studied, 25 systems are stable mostly because the induction contribution (%Ind > 50) and the other 29 are stable thanks to a balanced combination of electrostatic, induction and dispersion contributions. The complexes of B01 with all of the cations analyzed are located apart from the other points of the corresponding cluster, confirming that benzene is not a good choice for modeling the cation-π interaction in graphene fragments.
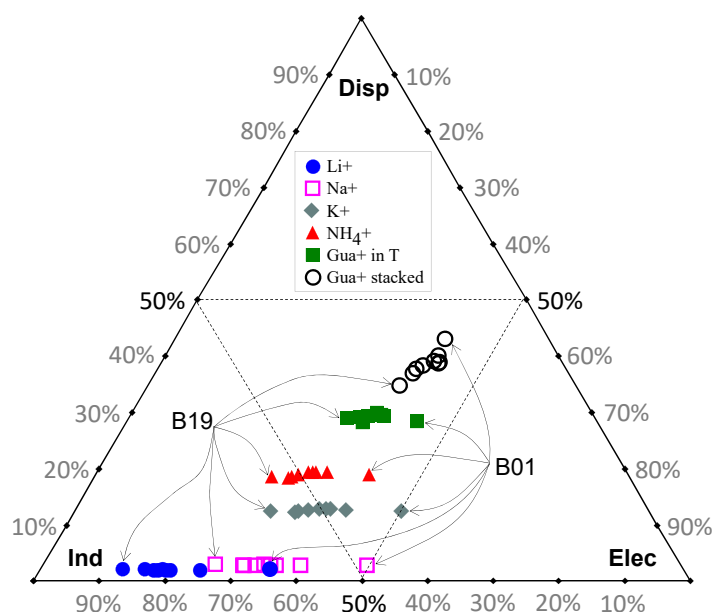
Figure 6. Contributions to the stability of the Electrostatic, Induction and Dispersion, calculated from the interaction energy analysis.

4. Conclusions

Cation-π interaction is theoretically studied in complexes formed between Li^+, Na^+, K^+, NH_4^+ and guanidinium cations and planar molecules with 1 to 19 fused benzene rings used as models of graphene fragments. Rigid scans performed at the TPSS+D3/ Def2TZVPP level of calculation show that all of the complexes studied are very stable and its interaction energy depends significantly on both, the size of the π-system and the nature of the cation. The energy analysis applied using the SAPT(DFT) method reveals that induction is the leading contribution to the stability of the complexes formed by Li^+ and Na^+ cations, even when electrostatic is also important in their complexes with small conjugated molecules. The contribution of dispersion is important in the complexes formed by K^+ and larger cations, especially in those formed by guanidinium in the stacked conformation. More than half of the complexes studied owe its stability to a balanced combination of electrostatic, induction and dispersion. Benzene (mainly) and anthracene are not good models for graphene fragments but following the tendencies observed with the molecules with four or more of benzene rings the results obtained can be extrapolated to extended π systems as graphene.

5. References

[1] Talotta, C.; Gaeta, C.; De Rosa, M.; Ascenso, J. R.; Marcos, P. M. and Neri, P., *Eur. J. Org. Chem.* **2016**, 158–167.

[2] Kumar, C. D.; Sharma, B. ; Soujanya, Y.; Chary, V. N.; Patpi, S. R.; Kantevari, S.; Sastry, G. N. and Prabhakar, S., *Phys. Chem. Chem. Phys.* 2014, **16**, 17266–17271.

[3] Nagy, E.; St.Germain, E.; Cosme, P.; Maity, P.; Terentis, A. C. and Lepore, S. D., *Chem. Commun*. 2016, **52**, 2311–2313.

[4] Zhao, C.; Toste, F. D.; Raymond, K. N. and Bergman, R. G., *J. Am. Chem. Soc.* 2014, **136**, 14409–14412.

[5] Spisak, S. N. ; Zabula, A. V.; Filatov, A. S.; Rogachev, A. Y. and Petrukhina, M. A., Angew. *Chem., Int. Ed.* 2011, **50**, 8090–8094.

[6] Carrazana-Garcia, J. A.; Rodriguez-Otero, J. and Cabaleiro-Lago, E. M., *J. Phys. Chem. B* 2012, **116**, 5860–5871.

[7] Dougherty, D. A., *Acc. Chem. Res.* 2013, **46**, 885–893.

[8] Arias, S.; Bergueiro, J.; Freire, F.; Quiñóá, E. and Riguera, R., *Small*, 2016, **12**, 238–244.

[9] Mahadevi, A. S. and   Sastry, G. N., *Chemical Review*, 2013, **113**, 2100-21.8.

[10] Xiu, X.; Puskar, N. L.; Shanata, J. A. P.; Lester, H. A. and Dougherty, D. A., *Nature* 2009, **458**, 534–537.

[11] R. R. Kumpf and D. A. Dougherty, *Science* 1993, **261**, 1708–1710.

[12] Hwang, D. S. ; Zeng, H. ; Lu, Q.; Israelachvili, J. and Waite, J. H., *Soft Matter* 2012, **8**, 5640–5648.

[13] Cabria, I.; López, M. J.; Alonso, J. A., *J. Chem. Phys.* 2005, **123**, 204721-1 – 204721-9.

[14] Kim, S. Y.; Lee, H. T.; Kim, K.-B., *Phys. Chem. Chem. Phys.* 2013, **15**, 20262−20271.

[15] Nerenberg P.S., Head-Gordon, T., *Curr. Opin. Struct. Biol.* 2018, **49**, 129-138.

[16] De Vivo, M.; Masetti, M.; Bottegoni, G. and Cavalli, A., *J. Med. Chem.* 2016, **59**, 4035−4061.

[17] Hjertenæs, E.; Nguyena A. Q. and Koch H., *Phys.Chem.Chem.Phys.* 2016, **18**, 31431-31440.

[18] Sun, P. Z.; Wang, K. L.; Zhu,   H. W., *Adv. Mater.* 2016, **28**, 2287–2310.

[19] Lábas, A.; Krámos, B.; Bakó, I. and Oláh, J., *Struct. Chem.* 2015, **26**, 1411–1423.

[20] Mecozzi, S.; West, A. P.; Dougherty, D. A., *Proc. Natl. Acad. Sci. U. S. A.* 1996, **93**, 10566–10571.

[21] Ngola, S. M.; Dougherty, D. A., *J. Org. Chem.* 1998, **63**, 4566–4567.

[22] Mecozzi, S.; West, A. P.; Dougherty, D. A., *J. Am. Chem. Soc.* 1996, **118**, 2307–2308.

[23] Singh, N. J.; Min, S. K.; Kim, D. Y.; Kim, K. S.; *J. Chem. Theory Comput.* 2009, **5**, 515–529.

[24] Carrazana-García, J. A.; Rodríguez-Otero, J. and Cabaleiro-Lago, E. M., *J. Phys. Chem. B* 2011, **115**, 2774–2782.

[25] Carrazana-García, J. A.; Cabaleiro-Lago, E. M. and Rodríguez-Otero, J., *Phys.Chem.Chem.Phys.* 2017, **19**, 10543–10553.

[26] Frisch, M. J.; Trucks, G. W.; Schlegel, H. B.; Scuseria, G. E.; Robb, M. A.; Cheeseman, J. R.; Scalmani, G.; Barone, V.; Menucci, B.; Petersson, G. A.; et al. *Gaussian 09*, Revision B.01; Gaussian, Inc.; Wallingford, CT, 2009.

[27] F. Neese, *Wiley Interdiscip. Rev.: Comput. Mol. Sci.* 2012, **2**, 73–78.

[28] Szalewicz, K., *Wiley Interdiscip. Rev.: Comput. Mol. Sci.* 2012, **2**, 254−272.

[29] Jansen, G., *Wiley Interdiscip. Rev.: Comput. Mol. Sci.* 2014, **4**, 127−144.

[30] Heßelmann, A.; Jansen, G.; Schütz, M., *J. Chem. Phys.* 2005, **122**, 014103.

[31] Misquitta, A. J.; Szalewicz, K., *J. Chem. Phys.* 2005, **122**, 214109.

[32] Werner, H. J.; Knowles, P. J.; Knizia, G.; Manby, F. R.; Schütz, M.; Celani, P.; Korona, T.; Lindh, R.; Mitrushenkov, A.; Rauhut, G.; Shamasundar, K. R.; Adler, T. B.; Amos, R. D.; Bernhardsson, A.; Berning, A.; Cooper, D. L.; Deegan, M. J. O.; Dobbyn, A. J.; Eckert, F.; Goll, E.; Hampel, C.; Hesselmann, A.; Hetzer, G.; Hrenar, T.; Jansen, G.; Kö, C.; Liu, Y.; Lloyd, A. W.; Mata, R. A.; May, A. J.; McNicholas, S. J.; Meyer, W.; Mura, M. E.; Nicklaß, A.; O'Neill, D. P.; Palmieri, P.; Peng, D.; Pitzer, K. P.; Reiher, M.; Shiozaki, T.; Stoll, H.; Stone, A. J.; Tarroni, R.; Thorsteinsson, T.; Wang, M. *Molpro, version 2012*, a package of ab initio programs, see http://www.molpro.net, 2012.

[33] Halkier, A.; Helgaker, T.; Jørgensen, P.; Klopper, W.; Koch, H.; Olsen, J.; Wilson, A. K., *Chem. Phys. Lett.* 1998, **286**, 243−252.

[34] Helgaker, T.; Klopper, W.; Koch, H.; Noga, J., *J. Chem. Phys.* 1997, **106**, 9639−9646.

[35] Cabaleiro-Lago, E. M.; Fernández, B.; Rodríguez-Otero, J., *J. Comput. Chem.* 2018, **39**, 93−104.

[36] Heßelmann, A.; Korona, T., *J. Chem. Phys.* 2014, **141**, 094107.

[37] Řezáč, J.; Hobza, P., *J. Chem. Theory Comput.* 2011, **7**, 685−689.